Chinese Chemical Letters 34 (2023) 108276

Contents lists available at ScienceDirect

Chinese Chemical Letters

journal homepage: www.elsevier.com/locate/cclet

Adhesive chitosan-based hydrogel assisted with photothermal antibacterial property to prompt mice infected skin wound healing

Shuang Cheng[a], Meng Pan[a], Danrong Hu[a,b], Ruxia Han[a], Lang Li[a,c], Zhongwu Bei[a], Yicong Li[a], Ao Sun[a], Zhiyong Qian[a,*]

[a] State Key Laboratory of Biotherapy and Cancer Center, and Collaborative Innovation Center for Biotherapy, West China Hospital, Sichuan University, Chengdu 610041, China
[b] Rehabilitation Medicine Center and Institute of Rehabilitation Medicine Key Laboratory of Rehabilitation Medicine in Sichuan Province, West China Hospital, Sichuan University, Chengdu 610041, China
[c] Department of Pediatric Surgery, West China Hospital, Sichuan University, Chengdu 610041, China

ARTICLE INFO

Article history:
Received 12 November 2022
Revised 22 February 2023
Accepted 27 February 2023
Available online 2 March 2023

Keywords:
Hydrogel
Adhesion
Photothermal therapy
Antibacterial
Wound infection

ABSTRACT

Bacterial infection of wounds is an escalating medical problem, issuing threats to both global public health and personal health. Photothermal antibacterial technology as a novel sterilization strategy has outstanding sterilization efficiency, high safety and low risk of emergence of drug-resistant bacteria. By combining inherent antibacterial activity and light-assisted antibacterial treatment, developing novel multifunctional dressings with synergistic high-efficiency antibacterial effects and also promoting wound healing possesses attractive advantages in the field of treating bacterial wound infections in clinical care. Herein, a multifunctional hydrogel formed by *in situ* photo-cross linking was designed and prepared by first grafting methacrylic anhydride as a photosensitizer onto chitosan, and then introducing oxidatively synthesized polydopamine (PDA). The physicochemical characterizations of the synthesized hydrogels demonstrated their tunability certainly associated with PDA concentration, including pore size, water swelling, rheological properties and *in vitro* degradability. In addition, the composite hydrogels exhibited good adhesion, anti-oxidation and photothermal properties due to the existence of PDA. Within 10 min upon exposure to 808 nm near-infrared (NIR) light irradiation, this hydrogel system displayed outstanding antibacterial activity against *Staphylococcus aureus* with almost 100% killing efficiency, of which rapid efficient sterilization plays a significant role in wound healing. Moreover, the hydrogel is capable of cytocompatibility and has low toxicity to murine fibroblasts (L929 and NIH/3T3). In the full-thickness wound defect infection model in mice, the wound closure ratio, inflammatory response, fibroblasts, neovascularization and epithelialization were measured. Animal experiments also reveal that the hydrogel assisted with NIR laser irradiation can inhibit effectively infection at an early stage and accelerate the wound healing process. In summary, this novel multifunctional injectable hydrogel exhibits excellent swelling capacity, bio-adhesion, antioxidant property, photothermal activity, efficient antibacterial property and facilitates skin healing, which has great promising application as a medical dressing biomaterial in infected wound care fields.

It is surely essential for skin as the largest organ of the human body to regulate human multiple activities and functions, including but not limited to sense of external environment, thermoregulation and protection from pathogens [1]. As a consequence of various factors including physical damage resulting from daily activities, prolonged exposure to overload, traumatic, burns and diverse diseases, the wholeness of the skin tissue, can be impaired or defects can be generated, which is defined as a wound [2]. Owing to long period required for the injured tissue repair and regeneration, and the morbidity affiliated with bleeding, risk of sepsis and scar formation, wound issues have become one of the major clinical problems worldwide, accompanied with emotional and financial strain to patients and their families and economic burden to the healthcare system [3,4]. According to statistics, the loss of wounds to the United States exceeds $25 billion every year, and the economic loss to developing countries is even more serious [5]. Once the integrity of the skin is damaged by acute or chronic injuries,

* Corresponding author.
E-mail address: anderson-qian@163.com (Z. Qian).

https://doi.org/10.1016/j.cclet.2023.108276
1001-8417/

the body can trigger a multi-step and dynamic processes around the wound sites, including the four stages of hemostasis, inflammation, proliferation and remodeling, which can result in restoration of the skin's structural integrity and barrier function [6]. Nevertheless, any adverse factors in the wound healing process like the mass generation of reactive oxygen species or the bacterial infections can lead to the formation of chronic non-healing wounds or abnormal scar [7]. Especially for open wounds on the human body, their surfaces are very susceptible to be infected by various bacteria, which can hinder the healing process and lead to life-threatening complications [7,8]. Therefore, reducing the probability of wound infection is the key to promoting wound tissue recovery, and it also becomes one of the hot issues in the field of wound treatment and care worldwide.

There are a large number of therapeutic strategies used for wounds, comprising auto/allograft and xenograft [9], tissue engineering [10,11], photothermal/photodynamic therapy (PTT/PDT) [12,13], electrical stimulation therapy [14,15], compress therapy [16,17], topical drug delivery [18] and hyperbaric oxygen therapy [1,19]. Wound dressings play an indispensable role on wound healing regardless of the type of wound or wound care selected strategy, which can also be considered as an easy and efficient one by covering the wound [1,20]. Traditional wound dressings (cotton, bandages and gauze) are used to stop bleeding and protect wounds from contamination, while the hemostatic and antibacterial effects that can be achieved are unsatisfactory [21]. Moreover, they could hardly suit with the open wounds and present no active effect on wound healing [1]. These dressings adhered to the skin tissue often need to be replaced frequently, leading to dehydration, infection and second injury [4]. In contrast, modern biomaterial-based wound dressings integrate multiple functions, which have been tested and approved by wound clinicians during the last 40 years [22]. Modern medical dressings essentially comprise film, foam, sponge, electrospun nanofiber, hydrogels and hydrocolloid types [20,23]. The hydrogel with special characteristics exhibits the most promising potential to develop into the ideal dressing among all of them [24]. In addition, for the purpose of adapting to the wound complex shapes, such as wrinkles or grooves, *in situ* forming hydrogel with formation of respectable fit can not only maintains a moist environment for wound recovery, but also provides good patient compliance [25].

Although these technologies have great outstanding effects on treatment of acute and small-scale traumatic wounds, there appears to face significant barriers in addressing the poorly healing effect and clinical complexity of large area burns, infected wounds and chronic wounds [5]. Bacterial infection has always been a great challenge to human health, usually existing in wounds on human body surfaces [26]. In particular, *Staphylococcus aureus* (*S. aureus*) considered as one of most common causes of burns and wounds, can bring about localized purulent infection, and even pneumonia, sepsis, and other systemic infections [27]. Currently, antibiotics are the most common treatment to anti-infection, which has been in use for nearly 80 years since it was first discovered [28]. Nevertheless, overuse or abuse of antibiotics has caused the evolution of multi-antibiotic resistant bacteria, which has become a worldwide issue in medical practice [29]. It is evaluated by the Center for Disease Prevention and Control that at least 2.8 million people evolve antibiotic-resistant infections and more than 35,000 people die in the U.S.A. every year [30]. Numerous novel antibiotic-free strategies have been reported to kill bacteria, of which PTT is one of the most appealing emerging means and can damage bacteria through various thermal effects [27,31]. PTT, comprehended as a safe and efficient strategy, can battle against infections by means of the heat generated from agents under the irradiation of near-infrared (NIR) light (covering 700 nm to 1400 nm) [32]. Compared to ultraviolet light (UV) and visible light, NIR light can penetrate deeper tissue without apparent damage to surrounding healthy tissues, which makes it possible for PTT to precisely and remotely control bactericidal treatment [33]. Polydopamine (PDA) is a kind of melanin analog with various outstanding properties including high photothermal conversion efficiency and stability, low cytotoxicity, and secondary chemical reactivity, making it a potential excellent photothermal therapeutic agent for the treatment of cancer and bacterial infections [34–38]. Similar to mussel secreted protein (DOPA) in structure, dopamine possesses various functional groups such as catechol, amine, imine, *etc.*, contributing to strong adhesion with almost all inorganic/organic/metal surfaces, *via* forming strong covalent or non-covalent bonds, and applications in the wound as hemostatic agents and adhesives [38–40]. Like a double-edged sword, the existence of a large number of active moieties on the surface makes it extremely easy for PDA to aggregate together, which will decrease the light absorbance and photothermal conversion efficiency, eventually severely hindering the practical application of PDA-based PTAs [38]. In general, the strong adhesive strength, degradability, low cytotoxicity, remarkable biocompatibility and effective antibacterial activity make PDA ideal for wound dressing applications [27,41].

The single use of PTT exists an inherent limitation that excessive temperature can damage the surrounding normal tissues, and therefore it is not capable of completely killing bacteria on its own. In order to improve the sterilization efficiency, PTT is commonly synergized with other antibacterial strategies for sterilization, such as metal ion and drug release, electrostatic adsorption bacteria [35,38,42]. Chitosan (CS), as the only alkaline polysaccharide with cations in nature, with positively charged amino group on its main chain, has a strong attraction to the negatively charged bacterial cell wall, which can form electrostatic adsorption between them to kill the bacteria by destroying the cell wall [20]. In addition to antibacterial and hemostatic activities, chitosan also possesses excellent biocompatibility and degradability, which has been approved by Food and Drug Administration (FDA) to applications for commercial dressings and widely reported as promising dressing materials for wound and burn treatments [32,43,44]. In terms of defense against infection, hydrogels with inherent antibacterial property have been widely developed as effective antibacterial agents with minimum by-effects [32]. Moreover, combined with other antibacterial strategies, chitosan-based materials are often capable of synergistic antibacterial activities in enhancement of specificity and efficiency [45]. However, most of the previously reported modified CS-based hydrogels have poor adhesion properties, which can severely hinder the integration with the surrounding tissue surface, further making wounds susceptible to bacterial infections and leading to prolonged wound healing [41,46]. Therefore, it is of great significance to develop a biomaterial with both effective antibacterial activity and strong adhesion property for the treatment of wound infection.

Herein, an injectable hydrogel that is rapidly cross-linked by UV light is designed by combining the unique advantages of CS and PDA, depending on grafted double bonds of chitosan modified by methacrylic anhydride. The obtained injectable hydrogel methacrylated chitosan (CSMA)/PDA shows spongy structure, which can not only afford the material proper swelling property for tissue exudate absorption but also overcome the limitation of PDA easy to aggregate. By incorporating photothermal agent polydopamine, the hydrogel CSMA/PDA also possess improved rheological, adhesion properties and unique antioxidant properties. In addition, hydrogels capable of excellent photothermal performance possess outstanding *in vitro* antibacterial capability against *S. aureus* under NIR laser irradiation, synergistic with inherent antibacterial activity of chitosan. Cytocompatibility of the hydrogel was estimated by co-culturing with mouse fibroblasts (L929 and NIH/3T3 cells). By means of establishment of a full-thickness wound defect infection

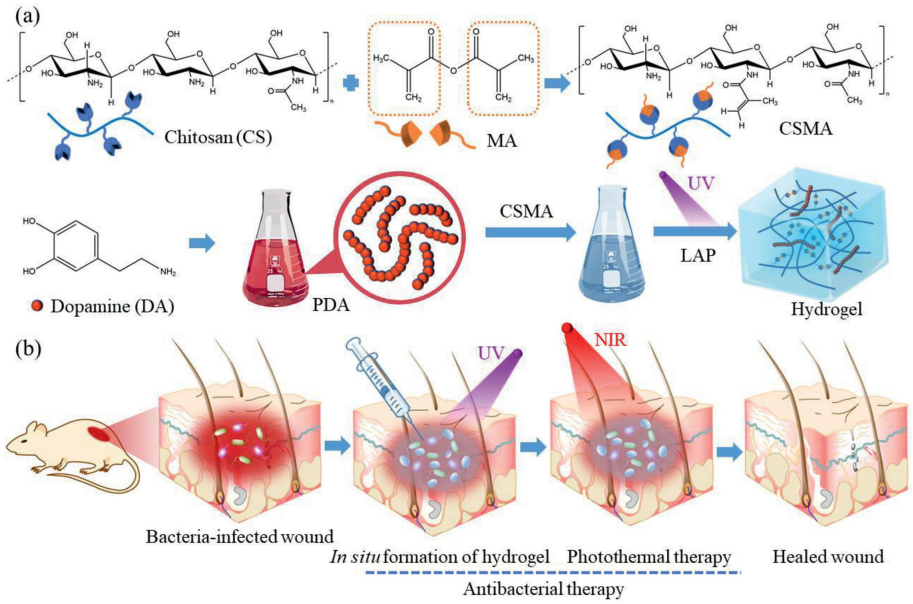

Fig. 1. Schematic illustration of preparation of CSMA/PDA hydrogel and its application assisted with photothermal antibacterial property to prompt mice infected skin wound healing: (a) Diagram of the method used to prepare CSMA/PDA injectable hydrogels. (b) The constructed hydrogel dressing can promote wound healing by synergistic photothermal antibacterial.

model in mice, the favorable effect of hydrogel CSMA/PDA on promoting infected wound healing was carried out in term of wound contraction, inflammatory response, fibroblasts, neovascularization, and epithelialization. From all of these results, it can be concluded the prepared biocompatible and multifunctional hydrogel has great application potential in infected wound healing fields.

The process for preparing CSMA/PDA hydrogels used as wound healing is illustrated in Fig. 1. To begin with, the amino group of the CS is modified with methacrylic anhydride by amidation reaction to obtain CSMA. Following this, PDA is synthesized by oxidative polymerization. As a final step, CSMA and PDA were dissolved in phosphate buffered saline (PBS), and the photoactivator lithium phenyl(2,4,6-trimethylbenzoyl)phosphinate (LAP) was added to form hydrogel CSMA/PDA rapidly by irradiation with UV. The resulting adhesive antibacterial hydrogel is used as a wound dressing during wound repair.

The degree of methacrylate modification of CS was determined by ^{1}H NMR spectroscopy. The ^{1}H NMR spectra (Fig. S1a in Supporting information) show the characteristic peaks of CS glucosamine rings (around 2.8–4.0 ppm, 6H) [47]. With the methacrylated CS, additional peaks are evident at 5.9 and 6.4 ppm representing the alkenyl double bond from the methacrylic anhydride moiety conjugated to CS [48]. The peaks from 1.9 ppm (Hc) to 2.1 ppm (Hd) correspond to the methyl protons of methacrylic anhydride residues and methyl protons of *N*-acetylglucosamine [48]. According to the previous method [48], the degree of methacrylation was determined by the ratio of mean area of the proton peaks of the methacrylate groups (δ = 5.9–6.4 ppm) relative to that of the CS glucosamine ring protons (δ = 2.8–4.0 ppm) and calculated to be approximately 22.37% for the synthesis with methacrylic anhydride (MA) conjugated to CS. Besides, the degree of acetylation of CS before modification was found to be 12% by ^{1}H NMR and these spectral data are in good agreement with the report [48].

The Fourier-transform infrared (FT-IR) spectrum of CS and CSMA were shown in Fig. S1b (Supporting information). The spectra showed characteristic absorption bands at 1026–1151 cm^{-1}, belonging to amine C–N stretch from CS. The evident increase in the intensity of the absorption bands at 2850 and 2930 cm^{-1} was observed in the spectra of the methacrylated products, being corresponded to alkyl C–H stretch both of CS and methacrylate groups. Several new peaks at 1653, 1538 and 1319 cm^{-1} appeared in the spectrum of CSMA, which should be attributed to amide type I (C=O stretching), II (N–H deformation and C–N stretching) and III groups, due to the new conformation of amide. The result of attenuated total reflection Fourier-transform infrared (ATR-FTIR) spectra further verified the successful methacrylation of CS.

The porous structure of the hydrogel not only is beneficial to the exchange of oxygen and the transportation of nutrient but also provides the capabilities of assimilating the exudates from the wound and maintaining suitable moisture [49]. The inner microstructures of freeze-dried hydrogels were revealed by scanning electron microscopy (SEM) (Figs. S2a–d in Supporting information). All of the four hydrogels exhibit a sponge-like interconnected porous structure and are regularly distributed, compared with irregular microstructure of some other chitosan hydrogels [50]. As shown in Figs. S3a–d in Supporting information, the average pore size varies from 150.0 μm for CSMA/PDA-1, to 228.4 μm for CSMA/PDA-2, and to 254.6 μm for CSMA/PDA-4, suggesting that the content of PDA significantly affect the three-dimensional architecture of the hydrogels, especially the pore size. Noticeably, the pore size of CSMA hydrogel was larger than that of CSMA/PDA-1 hydrogel. The CSMA hydrogel was covalently cross-linked by free radical polymerization of double bonds under UV light. With introducing polydopamine into hydrogels, the polydopamine may interact with the positive-charged amine groups on CSMA chains *via* cation-π interaction and hydrogen bonds [51], contributing to the increasement of the crosslinking density and the reduction of the pore size. Moreover, the interaction between PDA and the amine groups on CSMA chains gradually increased with the increase of PDA content in the hydrogels, which may restrict the movement of chitosan chains, resulting in hindering the formation of covalent cross-links from photo-induced free radical polymerization.

Three-dimensional network structure of hydrogel can supply nutrition and provide channels for waste to be discharged. Generally, the three-dimensional network structure can be partially understood by examining equilibrium swelling behavior, which is affected by the gel composition and crosslink density [52]. Hence, equilibrium swelling ratios offer a valuable means of understand-

ing hydrogels' internal structure. In regard to infected wounds, a swellable hydrogel can absorb the bacterial fluid from the wound site, and then operate as a wound antibacterial therapy through the use of photothermal therapy as well as inherent antibacterial properties. Fig. S4a (Supporting information) shows that all hydrogel samples exhibited fast swelling during the initial swelling time period (<1 h). The equilibrium swelling ratios of CSMA/PDA-1, CSMA/PDA-2 and CSMA/PDA-4 hydrogels tended to increase with decreasing cross-link density from 14.60, 16.77 to 18.81, respectively. While equilibrium swelling ratios of hydrogel CSMA/PDA-2 and CSMA were somewhat different, the difference was not statistically significant ($P > 0.05$). In agreement with the SEM results, hydrogels with a high crosslink density have a low swelling ratio since it is difficult for water molecules to enter the inner side [52].

Determining whether a hydrogel is suitable for degradation has also been considered an important indicator of biomaterial performance. This degradation behavior was assessed in 37 °C PBS buffer (pH 7.4) by simulating a physiological environment *in vivo* (Fig. S4b in Supporting information). As soon as the samples were immersed in PBS for 5 days, they showed a significant loss of mass, and after that the degradation rate slowed down, which might result from unreacted CSMA and PDA residuals in the network diffusing out of the hydrogel matrix and causing the higher weight loss of the hydrogels in the first 5 days. The minimum mass retention of 52.22% was observed for the CSMA/PDA-4 hydrogel after 25 days. Upon decreasing the concentration of PDA, the remaining weight ratio also increased from 61.37% to 65.97% and 69.67% for the CSMA/PDA-2, CSMA/PDA-1 and CSMA hydrogels, respectively ($P < 0.05$), which was consistent with that of SEM. The CSMA hydrogel network is formed by the strong chemical interaction of covalent crosslinks, resulting in a slower degradation rate. Despite that, the chemical cross-linking of double bonds on chitosan is hindered with the introduction of polydopamine, and the physical interaction between the polymers is relatively weak, which is more susceptible to the influence of the external environment in PBS buffer, giving rise to the three-dimensional network structure of the hydrogel destroyed. To sum up, it is indicated that the CSMA/PDA hydrogel has a tunable degradation rate and good degradability, which is expected to fit the necessary requirements of skin tissue regeneration and repair.

The rheological behavior of the hydrogel must coincide with the following requirements: (i) its dynamic elastic modulus (G′) must be some extent independent of the frequency of distortion and (ii) G′ must be larger than the loss modulus (G″) at all frequencies [53].

These two characteristics are observed in the dynamic frequency sweep measurement results of Fig. S4c (Supporting information), where G′ and G″ are depicted as a function of frequency for hydrogel CSMA and CSMA/PDA. With increasing frequency, the G′ and G″ of the CSMA hydrogel significantly changed. The measured average G' of hydrogel CSMA, CSMA/PDA-1, CSMA/PDA-2 and CSMA/PDA-4 were 466, 1313, 8011 and 1522 Pa, respectively. Compared with these CSMA/PDA hydrogels, CSMA hydrogel exhibited the lowest G′ which means that the supplement of PDA could strengthen the mechanical property of the hydrogels. Additionally, the value of G″ was permanently less than that of G′, suggesting that CSMA/PDA hydrogels exhibit a comparatively structure and some viscoelasticity, and could resist a certain frequency of interference [21]. In conjunction, the physiochemical properties of CSMA/PDA hydrogels could be delicately modulated *via* altering the PDA amount, which is in accordance with the previous report [54].

Seamless wound treatment offers dominant position over traditional wound dressings [55]. It is very worthy of attention for wound closure to possess adhesiveness, for the reason that adhesive hydrogels can spontaneously adhere to the required site to combine with healthy tissues. Consequently, this kind of adhesive hydrogel not only acts as a scaffold during treatment, but also prevents fluid in or out by serving as an adhesive, hemostat or sealant [56–58]. The adhesion performance of these hydrogels relative to skin was evaluated by means of a lap-shear measurement (Fig. S4d in Supporting information). It was worth noting that the CSMA hydrogel without PDA also exhibited adhesion ability in Figs. S4e and f (Supporting information). The possible explanation was that electrostatic interaction, H-bonding as well as hydrophobic interaction were formed between CS and phospholipids on the cell membranes to supply the hydrogel with certain adhesive strength [43,59]. It could be also observed that the adhesive strength increased with the increasing concentration of PDA (Fig. S4f), due to the covalent bonds between the amino/thiol groups on PDA and porcine skin, as well as the physical interactions [56]. Nevertheless, it is also found that the adhesive strength of the CSMA/PDA-4 hydrogel with the maximum PDA content decreased slightly, in comparison to that of CSMA/PDA-2 hydrogel. There may be one explanation for this result that the higher content of PDA interacting with the chitosan chains on the hydrogel resulted in a limited mobility of polymer chains at adhesion interface to form incompatible contact with the tissue surfaces [59]. This CSMA/PDA-2 hydrogel with optimal adhesion strength (36.5 kPa) overcomes the limitation of previously reported non-adhesive CS-based hydrogel and can compare with most of the fibrin glue on the market (2–40 kPa), which could be appropriate for sealing skin wound [46,60].

Free radicals play a crucial role in all phases of wound healing [61]. It has been proved that topical applications of free radical-scavenging materials can accelerate wound repair, as antioxidants can coordinate the overproduction of reactive oxygen species (ROS) to prevent these species from adversely affecting [55,62]. 2,2-Diphenyl-1-picrylhydrazyl (DPPH) has been broadly utilized to estimate the free radical scavenging efficiency of numerous antioxidant substances. For the purpose of evaluating the antioxidant properties of the prepared dressings with introduction of PDA, their capability to scavenge the stable DPPH free radicals was investigated by means of monitoring the DPPH radical absorption peak at 517 nm (Fig. 2). The DPPH radical can be converted into the corresponding colorless hydrazine (DPPH–H) by the antioxidant, thereby recording the decay of the visible band of DPPH by means of monitoring the H-transfer reactions by ultraviolet–visible spectrophotometry (UV–vis) [63]. As shown in Fig. 2a, after the addition of PDA, the peak at 517 nm was sharply decreased with higher concentrations of PDA. Apparently, the scavenging ratio of the DPPH free radicals increased with higher concentrations of PDA, accompanied with a significant color shift from deep purple to pale-yellow (Fig. 2b). Quantitatively, after 160 min, the free radical scavenging rate of the CSMA/PDA-4 scaffold reached 76.57% in Fig. 2c. These results indicated that the CSMA/PDA hydrogels possess strong antioxidant ability, owing to the conversion of catechol groups of PDA to benzoquinone groups [64]. Summarily, the above results demonstrated the free radical scavenging ability of CSMA/PDA scaffolds, which will be beneficial for the regeneration process of skin tissue.

It has been generally accepted that photothermal ablation as a safe and efficient strategy is capable of preventing infections on the basis of the heat engendered by photothermal agents under NIR irradiation (700–1400 nm) [65]. To evaluate the photothermal performance of the hydrogel CSMA/PDA, the photothermal heating curves of the hydrogels were measured during 808-nm laser irradiation. As such, the several hydrogels with different PDA concentration and power of NIR laser were set as variables to assay the photothermal properties of CSMA/PDA hydrogels (Figs. 3a–c). The chitosan hydrogel without polydopamine showed faint temperature increase after 10 min NIR irradiation (1.0 W/cm^2). Besides, the equilibrium ΔTs gradually increased from 15.1 °C to 26.3 °C when increasing the polydopamine content, revealing a photother-

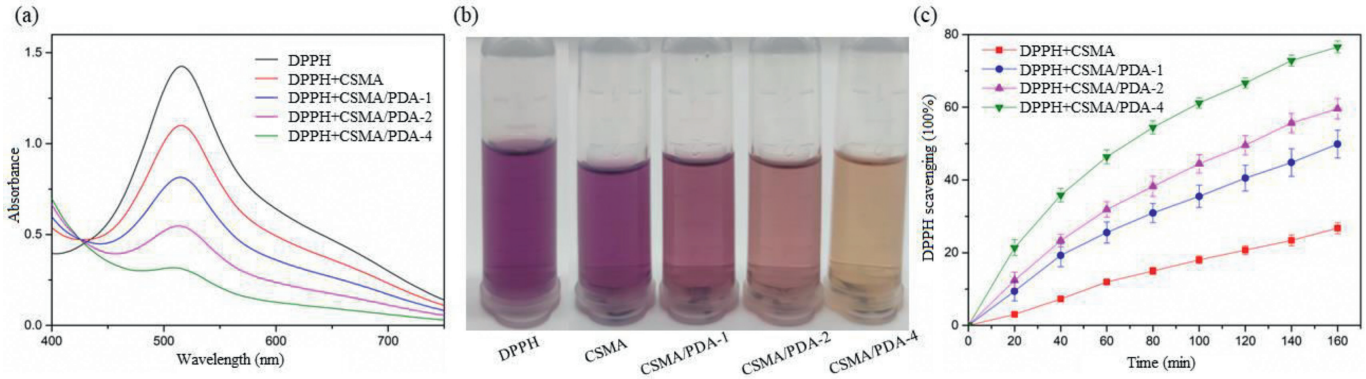

Fig. 2. (a) UV–vis spectra of the DPPH reaction with hydrogel scaffolds after 160 min (From top to bottom, DPPH, CSMA, CSMA/PDA-1, CSMA/PDA-2 and CSMA/PDA-4). (b) The image of the DPPH solution reaction with hydrogel scaffolds after 160 min. (c) DPPH scavenging efficiency of the hydrogel scaffolds at different time points ($n = 4$). All experimental results were expressed as a mean ± standard deviation (SD).

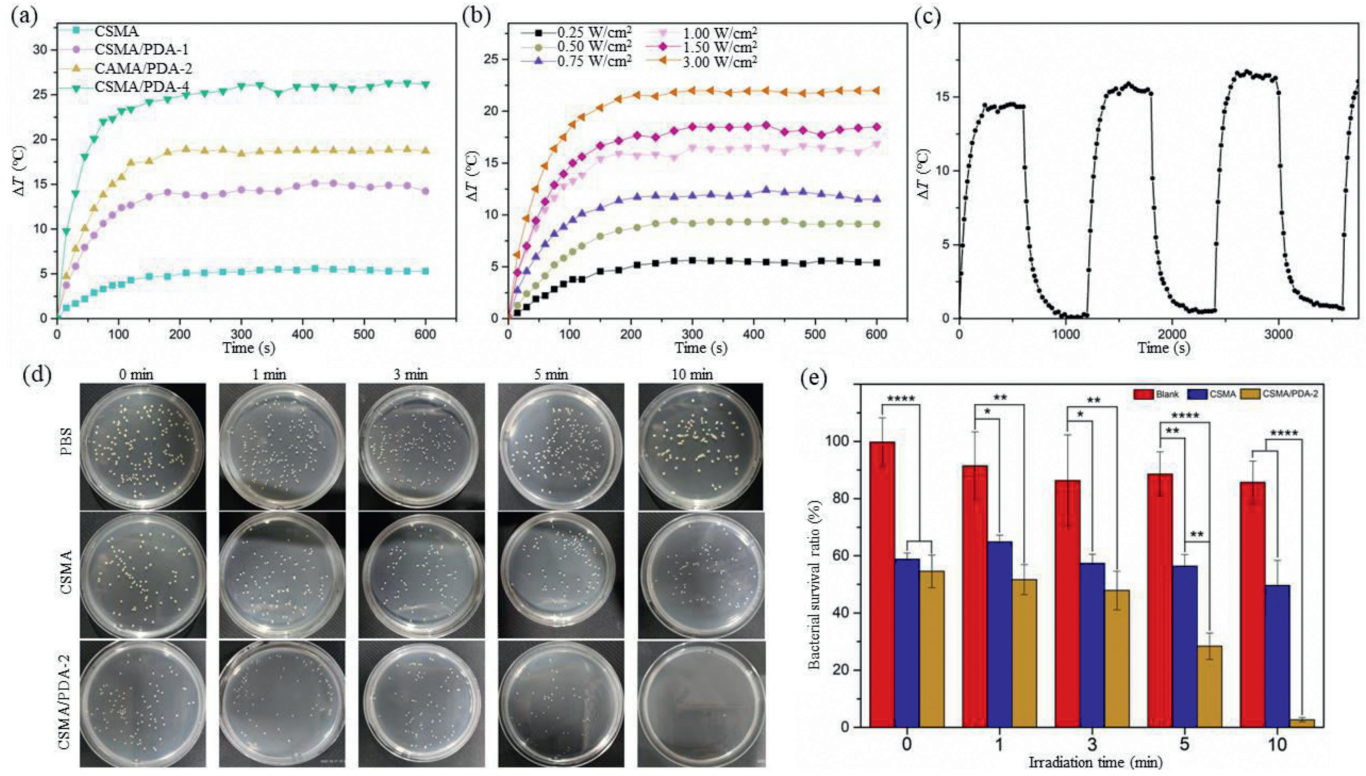

Fig. 3. (a) ΔT-NIR irradiation time curve of the hydrogel under irradiation with a power density of 1.0 W/cm^2. (b) ΔT-NIR irradiation time curve of the CSMA/PDA-2 hydrogel under irradiation with a power density of 0.25, 0.50, 0.75, 1.00, 1.50 and 3.00 W/cm^2. (c) ΔT-NIR irradiation time curve of the CSMA/PDA-2 hydrogel irradiated for three on/off cycles (1.0 W/cm^2). (d) Photothermal antibacterial behavior of CSMA and CSMA/PDA-2 hydrogels against *S. aureus* under NIR laser irradiation with a power density of 1.0 W/cm^2 for 0, 1, 3, 5 and 10 min. (e) Bacterial survival ratios of *S. aureus* as a function of NIR laser irradiation time ($n = 3$). All experimental results were expressed as a mean ± SD. Differences were considered significant if $P < 0.05$ ($^*P < 0.05$, $^{**}P < 0.01$, $^{****}P < 0.0001$).

mal effect of hydrogel CSMA/PDA dependent on polydopamine concentration. Moreover, when changing the NIR light intensity from 0.25 W/cm^2 to 0.5, 0.75, 1.0, 1.5 and 3.0 W/cm^2, the ΔTs of CSMA/PDA-2 gradually increased from 9.4 °C to 12.4, 16.9, 18.7 and 22 °C. From these results, it was indicated that the prepared CSMA/PDA hydrogels can efficiently convert the NIR light into heat and possess adjusted photo-thermal capability. As detected in Fig. 3c, after three light on-off cycles, the temperature increasement of CSMA/PDA-2 hydrogel did not change significantly, reflecting the admirable photothermal stability of the hydrogel CSMA/PDA. The controllable photothermal effect and stability make it possible for CSMA/PDA hydrogels to be used as a dressing *in vivo* with anti-infection and wound healing properties. Given the findings of adhesion tests and photothermal curves of CSMA/PDA hydrogels, CSMA/PDA-2 hydrogel was selected for subsequent experiments to ensure excellent adhesion properties and photothermal conversion capabilities of utilizations in wound dressing.

Bacterial infections can prevent skin wounds from healing, and *S. aureus* (a Gram-positive bacterium) is the most typical among these bacteria isolated from infected wounds [66,67]. The bacterial proteins and enzymes could be denatured when exposed high temperature ≥45 °C, bringing about the bacterial death [65]. In consideration of the prepared hydrogel's photothermal capacity, the NIR-assisted antibacterial properties of CSMA/PDA-2 against *S. aureus* were measured to determine whether the nearby heat generated by the hydrogel CSMA/PDA under NIR irradiation could effec-

tively sterilize (Figs. 3d and e). The hydrogel CSMA and PBS were used as the control group. The number of bacterial colonies for the experimental groups of CSMA/PDA-2 hydrogels assisted with photothermal treatment were significantly decreased, compared with control groups, implying outstanding bacterial killing effects. When NIR laser irradiated for 1 min, the bacterial survival ratio of the hydrogel containing PDA showed a significantly downward trend ($P < 0.05$), and the bacterial survival ratio of PBS, hydrogel CSMA and hydrogel CSMA/PDA was 91.5%, 64.8% and 51.68%, respectively. On the basis of this, the significant decay trend of bacterial survival ratio was displayed with the irradiation time prolonged. When the NIR laser irradiation time was increased to 10 min, the bacteria were almost entirely killed in the CSMA/PDA hydrogel experimental group. In contrast, almost no reduction in bacterial survival occurred in the PBS group, demonstrating that pure NIR imposed no apparent damage to bacteria. Without NIR laser irradiation, the antibacterial ratios of hydrogels CSMA and CSMA/PDA were significantly higher than that of the PBS control groups ($P < 0.05$), due to the inherent antibacterial activity derived from CS and PDA [68,69].

The antibacterial mechanism of the CSMA/PDA hydrogel is attributed to the following three points. In the first place, the electrostatic interactions between protonated amino groups on chitosan and negatively charged bacterial cell membranes can effectively kill bacteria on the surfaces of the hydrogels [68,70]. There is one more point, the structure of the bacterial cell membrane can be damaged by PDA through the chelation of ions/proteins and the electrostatic effect [69]. The last but not the least, the excellent NIR–assisted photo-thermal ability of polydopamine in hydrogel CSMA/PDA can increase the temperature under the irradiation of NIR light, further significantly promoting its antibacterial capacity for gram-positive bacteria even when bearing a challenge of 10^8 CFU/mL bacteria [51,70]. The hydrogel containing PDA component has been indicated to possess synergistic antibacterial effects including excellent *in vitro* NIR photo-thermal antibacterial performance and inherent antibacterial property of chitosan, showing great potential for wound dressings.

Good biocompatibility is an important property of hydrogels as wound dressings, with the hydrogels intended to be delivered (injectable) to host cells [71]. For the purpose of avoiding unexpected incompatible host responses, it is essential to evaluate their toxicity and biocompatibility to mammalian cells. In general, it is suitable to test the cytotoxicity in considerable amount of material using MTT [72]. In this test, the cytocompatibility of the composite hydrogel was estimated using L929 and NIH/3T3 fibroblast cells as the model normal cells *via* the standard MTT assay method. In addition, L929 and NIH/3T3 cells incubated with a culture medium were selected as control, whose cell viabilities were defined as 100%. As illustrated in Fig. S5 (Supporting information), all the hydrogel groups showed high cell viabilities (>80%), while the cell viability of pure CSMA hydrogel group was the lowest compared with other groups. According to ISO 10993–5:2009, the reduction of cell viability by >30% is defined as a cytotoxic effect and as the assessment results of the cellular viability attained for the prepared hydrogels reached above 80%, coming to a conclusion that the materials are less cytotoxic [73,74]. Compared with the that of the pure CSMA hydrogel group, the L929 and 3T3 cell viabilities of the CSMA/PDA hydrogel groups were significantly improved, respectively, reaching more than 90%. In Fig. S5a, the cell viabilities of L929 were 97.60%, 96.52% and 97.70% after incubation in the CSMA/PDA hydrogel extract for 24 h at 37 °C, showing no significant difference compared to the control group ($P > 0.05$). As shown in the culture results of 3T3 cells of Fig. S5b, the cell viabilities were increased from 83.47% to 92.02%, 99.79% and 106.20% with PDA content of the CSMA/PDA hydrogels increased. This observation emphasize that the addition of PDA facilitated the improvement of cell viability of the hydrogels, demonstrating once again the advantages over the prepared CSMA/PDA hydrogel for application in wound dressings.

Since cell migration is essential for healing/regeneration of wound tissue, scratch assay *in vitro* as a simplified model of wound to evaluate the effect of extraction media from the hydrogel on proliferation and migration of L929 fibroblasts [75]. Fig. 4a show the photos of each selected field of view at representative time points, revealing that the extracts from hydrogels can fasten the scratch reparation process. The quantitative analysis of wound closure (Fig. 4b) showed that wound closure rate for the CSMA/PDA-2 hydrogel group was 25.39%, which is significantly higher than that of the control group (15.78%, $P < 0.05$) at 16 h. After 72 h of treatment, the wound closure rate of the CSMA/PDA-4 hydrogel treated group was the highest, reaching 76.38%, which was significantly higher than that of the control group by 12.98% ($P < 0.001$). Moreover, the CSMA/PDA-2 hydrogel and CSMA/PDA-4 hydrogel treated groups also had a significant increase ($P < 0.001$) compared with the pure CSMA hydrogel treated group (64.78%) after 72 h of culture. As a result, the scratch test analysis confirmed that extracts from the CSMA/PDA hydrogels can promote the migration and proliferation of fibroblasts, especially PDA that has been demonstrated to facilitate the improvement of cell viability in MTT.

In vitro results, it has been demonstrated that the hydrogel with injectability, biocompatibility, excellent antibacterial activity, and adhesiveness displayed promising application in wound closure and anti-infective treatment. The *S. aureus*-infected full-thickness-skin wound mouse model was established to assess the antibacterial effect and wound healing property of the hydrogel CSMA/PDA under NIR laser irradiation *in vivo* (Fig. 5). All animal experiments were carried out complied with the NIH Guide Concerning the Care and Use of Laboratory Animals and were approved by the Animal Experimentation Ethics Committee of Sichuan University, Chengdu, China. The skin infected wounds were treated with the CSMA/PDA-2 hydrogel and CSMA/PDA-2 hydrogel combined with NIR laser irradiation, and the infected wounds treated by Tegaderm commercial dressing and pure CSMA were determined as controls. During the treatment, the typical images of the wounds were recorded with a digital camera on days 0, 3, 7 and 14 (Fig. 5a). The wound contraction rate was calculated in accordance with a comparison of wound area in healing wound sites with that of initial wound sites on day 0.

Apparently, the wound healing effect of hydrogel CSMA/PDA-2 + NIR treatment group is noticeable, and no obvious wound could be observed after 14 days of treatment. On day 3, wounds treated with the hydrogels had a significantly greater percentage wound closure because of epithelialization compared with the Tegaderm dress only control (39.36%, 42.54%, 58.61% *vs.* 3.40%, respectively, $P < 0.0001$). On day 14, this trend kept going (43.66%, 55.10%, 69.58% *vs.* 11.02%, respectively, $P < 0.0001$). All wounds were decreasing in size and exhibited signs of scab formation on day 7, while accelerated wound closure was appeared among the hydrogel treatment groups on days 7 and 14. Moreover, there was an apparent sign of infection of the Tegaderm dress treatment group on day 7, containing exudate or purulent drainage. Compared with Tegaderm dressing group, other hydrogel groups presented smaller wound areas after 14 days of treatment ($P < 0.05$). In addition, the CSMA/PDA-2 hydrogel treatment group showed a higher wound healing rate for bacterial infected skin than pure CSMA hydrogel group after 14 days ($P < 0.05$). On the days 3, 7 and 14, the wound sites of hydrogel CSMA/PDA-2+ NIR group were much smaller than other only hydrogel treatment groups ($P < 0.05$).

In summary, the group treated with hydrogel CSMA/PDA-2 under NIR laser irradiation exhibited the highest wound closure among these groups, which confirmed that CSMA/PDA-2 hydrogel assisted with NIR irradiation possessed the fastest rate of wound healing. This might be owing to the inherent antibacterial activity

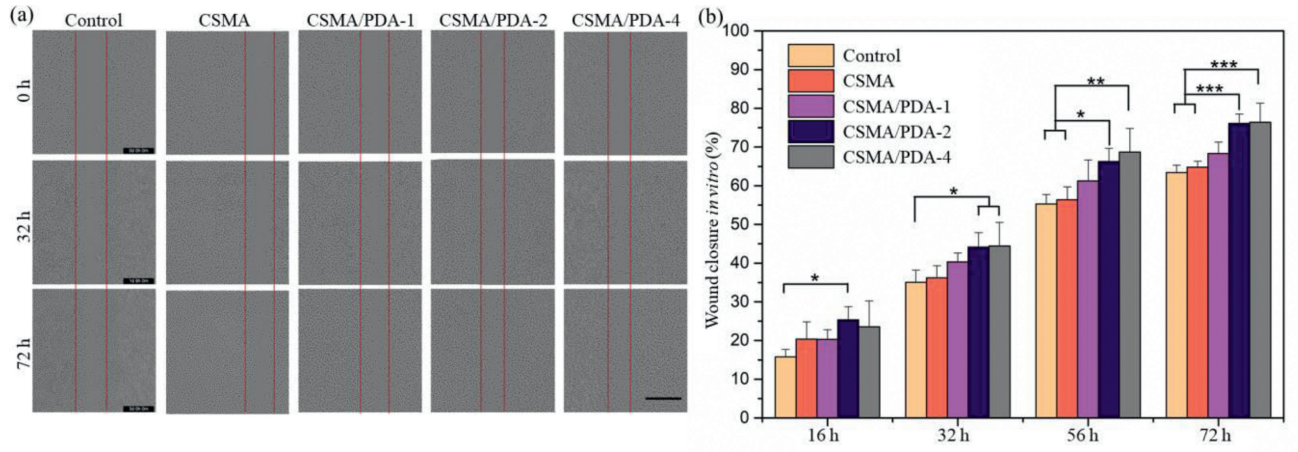

Fig. 4. Migration of L929 treated with hydrogels for different time *in vitro*: (a) Representative micrographs of scratch areas; the red line was added for better illustration of the scratch margin; (b) Statistical data of wound closure percentage *in vitro* ($n = 4$). All experimental results were expressed as a mean ± SD. $^{*}P < 0.05$, $^{**}P < 0.01$, $^{***}P < 0.001$. Scale bar: 500 μm.

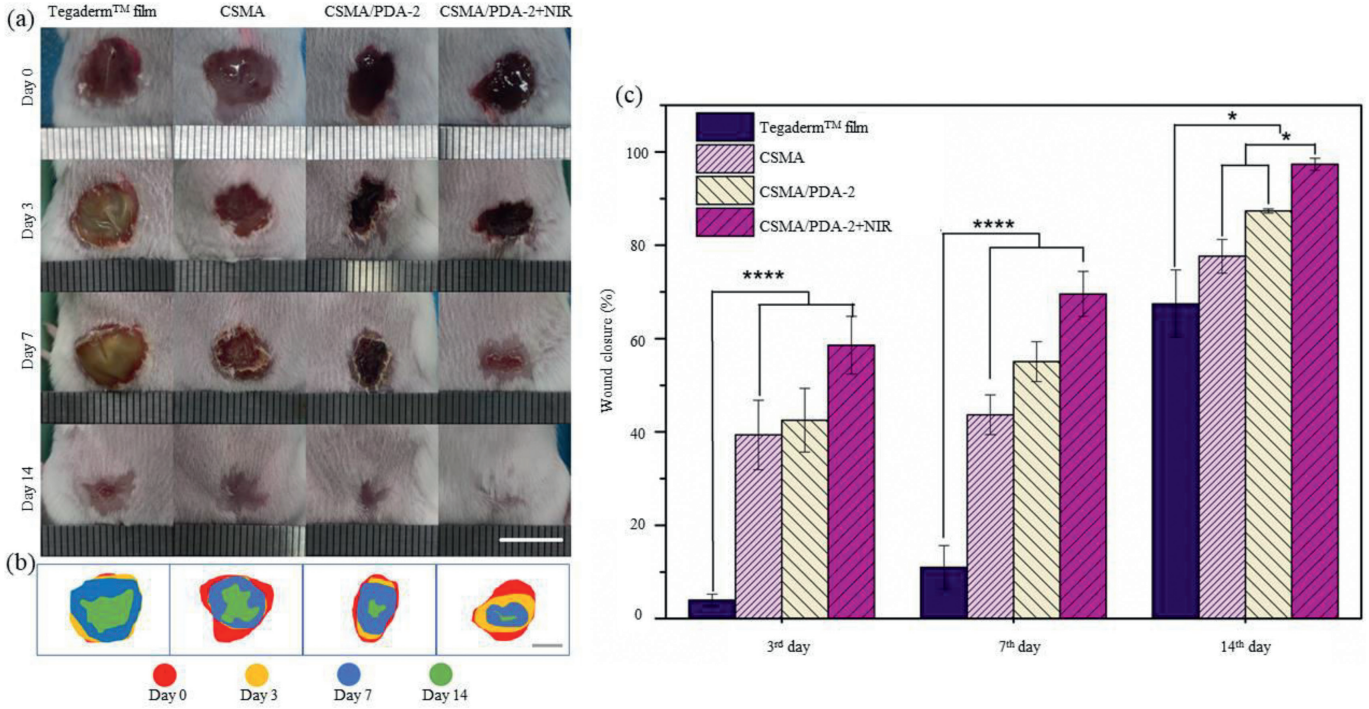

Fig. 5. (a) Representative photographs of wounds from days 0 to 14 of Tegaderm™ dressing, CSMA, CSMA/PDA-2 hydrogel, and CSMA/PDA-2 + NIR treatment. Scale bar: 10 mm. (b) Wound traces for different treatment days. (c) Evolution of wound area ratio for different treatment days ($n = 4$). All experimental results were expressed as a mean ± SD. $^{*}P < 0.05$, $^{****}P < 0.0001$.

of chitosan and polydopamine, assisted with NIR photothermal ablation, whose synergistic effect to enhance the antibacterial capacity of hydrogel on *S. aureus*, contributing to effectively kill bacteria and accelerate the wound healing process. Moreover, the moisture environment provided by hydrogel dressings and the ideal function of chitosan are both conducive to the healing of the wound.

In the process of wound healing, three important overlapping stages of inflammation, proliferation and remodeling can occur one after another [76]. After the death of mice on days 3, 7 and 14, the wound tissue was collected and histomorphological determination on wound regeneration in different phase was performed by hematoxylin-eosin staining (H&E).

Wound regeneration effect was evaluated by means of observing infiltration of inflammatory cells, fibroblast immigration, connective tissue synthesis and re-epithelization. On day 3, abundant macrophage infiltration appeared in all groups, including groups Tegaderm dressing and hydrogels. Attractively, compared with commercial dressing group and CSMA hydrogel group, inflammatory cell infiltration was fractionally inhibited and much more fibroblasts were clustered around the wound region treated with hydrogel CSMA/PDA-2 under NIR laser irradiation. On the 7th day, the group of hydrogel CSMA/PDA-2 with NIR laser irradiation exhibited complete re-epithelialization, with the thicker granulation tissue and more obvious fibroblast proliferation observed (Fig. 6). In comparison with the groups of film dressing and hydrogel CSMA, the CSMA/PDA-2 hydrogel treatment group demonstrated comparatively more granulation tissue with a number of fibroblast cells and microvessels around the impaired region, expediting continuous proliferation of the surrounding basal cells and migration to the wound surface to form new epithelial cells [77]. Relevant

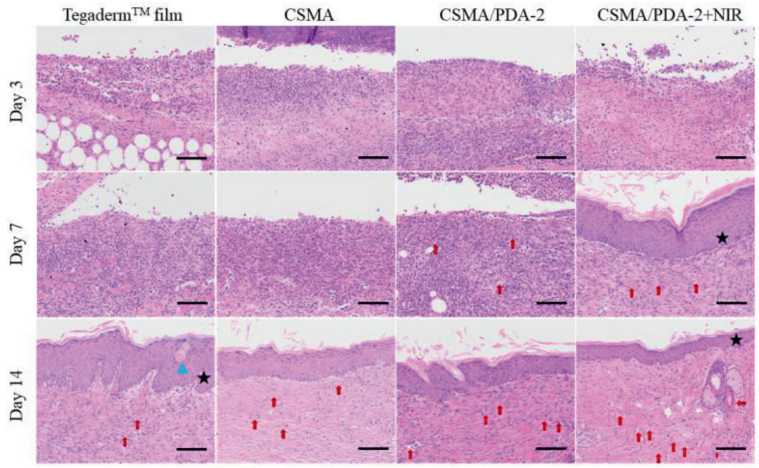

Fig. 6. H&E staining of skin tissues of mice wounds at different times (⋆: epidermis, ↑: blood vessel, ▲: necrotic tissue). Scale bar: 100 μm.

studies have shown that PDA with antioxidant effects is capable of promoting wound healing through controlling the level of reactive oxygen species at the wound sites during the wound repair process [55,77]. On the 14th day, epithelialization was complete in all the groups, while the film dressing group showed the thickest epidermis with necrotic tissue occurring inside the epidermis. On the contrary, the hydrogel treatment groups demonstrated a great number of tightly-connected connective tissues under the skin, including fibroblasts. Furthermore, the treatment group of the hydrogel assisted with NIR laser exhibited the thinnest skin with numerous angiogenesis and dermal appendices, concluding hair follicles and sweat glands. These properties, coupled with good cytocompatibility and adhesion property, suggest that the CSMA/PDA hydrogel dressing is a promising candidate for accelerating tissue repair during bacteria infected wound healing.

Collagen is a major component of the extracellular matrix (ECM), and its synthesis plays a crucial role in the skin wound healing process for it provides a scaffold for wound healing cells and regenerated blood vessels to facilitate wound healing [78]. Thus, in order to evaluate the formation of collagen fibers in postoperative wounds, Masson's trichrome staining of repaired tissue was conducted in this study and collagen was stained blue while the red color marked the muscle fibers and red blood cells. As presented in Fig. S6 (Supporting information), on day 7 after treatment, more newborn collagen fibers were observed granulation tissue of mice wounds in the CSMA/PDA-2 hydrogel treated groups, while the wound sites of the control group and CSMA group were almost not filled with newborn collagen fibers. In addition to the amount of collagen that can affect wound healing, its arrangement and distribution are also important criteria for evaluating wound healing, which can affect the strength of the new tissue [77,79]. During the 14 days post-surgery, the collagen content of all groups kept rising. However, most of the collagen in the control group was more disordered in arrangement, compared to that in the groups of the hydrogel CSMA and CSMA/PDA-2. It is worth to note that collagen fibers of the hydrogel CSMA/PDA-2 group treated with NIR laser irradiation were the best organized and the most highly ordered arrangement among all groups, and the structure of healing skin tissue in this group was similar to that of normal skin. Hence, these results indicate that CSMA/PDA-2 hydrogel assisted photothermal therapy can be conducive to the formation and arrangement of collagen to accelerate the wound healing.

It is necessary for wound healing to provide sufficient nutrients and metabolism for tissue repair and reconstruction, and wound neovascularization is the basis for providing nutrients [80,81]. Therefore, in the process of wound repair, the degree of wound healing will be greatly affected by the quantity and quality of angiogenesis [82]. In this study, the expression of CD31 on the surface of newly formed capillary endothelial cells was analyzed by immunohistochemistry to evaluate the wound healing effect of hydrogel-induced full-thickness skin defect wounds; the results are shown in Fig. S7a (Supporting information). On day 7 after trauma, almost no obvious neovascularization was seen in the control group, while a large amount of neovascularization was observed in all three hydrogel-treated groups. After 14 days of treatment, a large number of new blood vessels were also observed in the control group. However, compared with the control group, the new blood vessels in the hydrogel-treated group were larger in diameter and more mature. The CSMA/PDA hydrogel with NIR laser group had the highest number of vascular angiogenesis, compared with the hydrogels without NIR groups. In general, early vessels that form under high proangiogenic pressure are often immature, hyperpermeable, and dysfunctional, and their timely degeneration will be beneficial to avoid scarring and improve the quality of wound recovery [83,84]. These results demonstrate that CSMA/PDA hydrogel can synergize photothermal therapy to promote angiogenesis and maturation in infected wounds, thereby accelerating wound healing.

It has been revealed that an inflammatory response at the site of wounds can be inevitable and also affect the efficiency of wound healing, usually caused by internal factors and external factors (*e.g.* bacterial infection) [85]. To further illustrate the effect of CSMA/PDA hydrogel in promoting wound healing, interleukin-6 (IL6), as a sensitive inflammation factor induced by bacteria, was selected for immunohistochemistry to evaluate the skin wound repair on day 7 [86]. As shown in Fig. S7b (Supporting information), after 7 days of treatment, the expression of IL-6 in the control group was the highest, and there were a large number of inflammatory cells, which was consistent with the obvious bacterial infection observed macroscopically. Compared with the CSMA hydrogel group, the two experimental groups treated with CSMA/PDA hydrogel had significantly less IL-6 inflammatory factor, which indicated that the addition of PDA made the hydrogel have better anti-inflammatory effect. In conclusion, the UV-crosslinked CSMA/PDA hydrogel could effectively inhibit the inflammatory response and bacterial infection.

In summary, an adhesive injectable hydrogel CSMA/PDA that can combine the inherent antibacterial activity of CSMA with photothermal treatment of photothermal agent PDA was developed, exhibiting rapid, efficient and long-term antibacterial activ-

ity, which can successfully fight against *S. aureus* infection and promote wound healing *in vivo*. By the double bond grafted onto chitosan and polydopamine introduced, the hydrogel is rapidly crosslinked by ultraviolet light under the action of a photoinitiator, making the hydrogel capable of injectability and *in situ* hydrogel formation. Catechol groups of PDA as well as amino groups on chitosan can interact with tissue interfaces, endowing the CSMA/PDA hydrogels with excellent tissue adhesiveness. The introduction of polydopamine not only supplied the hydrogel with excellent antioxidant properties, but also enabled the hydrogel to have tunable properties, comprising pore size, water swelling, rheological properties, and *in vitro* degradability. The hydrogel with PDA was able to rapidly increase the ambient temperature under NIR laser irradiation, synergizing with the inherent antibacterial activity of chitosan to significantly enhance the antibacterial properties against *S. aureus*. Hydrogels with all these desirable traits in conjunction with good cytocompatibility accelerated wound healing rates in a full-thickness skin wound infection model in terms of healing rate, inflammatory response, neovascularization and epithelialization, and also improved wound healing efficiency. Overall, the new photo-thermal antibacterial hydrogel materials proposed in this study will grant a promising strategy for clinical infected wound repair, and may greatly promote the speed of infected wound repair and the quality of repair.

Declaration of competing interest

The authors declare that they have no known competing financial interests or personal relationships that could have appeared to influence the work reported in this paper.

Acknowledgments

This work was funded by the National Natural Science Foundation of China (Nos. U21A20417 and 31930067), and 1·3·5 project for disciplines of excellence, West China Hospital, Sichuan University (No. ZYGD18002).

Supplementary materials

Supplementary material associated with this article can be found, in the online version, at doi:10.1016/j.cclet.2023.108276.

References

[1] R. Yu, H. Zhang, B. Guo, Nano Micro Lett. 14 (2021) 1.
[2] S.H. Lu, M. Samandari, C. Li, et al., Sens. Actuators Rep. 4 (2022) 100075.
[3] A. Andrade, M. Egito, W. Vilela, et al., Biointerface Res. Appl. Chem. 12 (2022) 4463–4475.
[4] M.J. Gotlin, W. Catalano, J.P. Levine, K.A. Egol, Injury 53 (2022) 313–322.
[5] S. Das, A.B. Baker, Front. Bioeng. Biotechnol. 4 (2016) 82.
[6] S. Rathinavel, J. Indrakumar, P.S. Korrapati, S. Dharmalingam, Colloids Surf. A 637 (2022) 128185.
[7] W. Elloumi, A. Mahmoudi, S. Ortiz, et al., Biomed. Pharmacother. 146 (2022) 112574.
[8] B. Li, H. Li, H. Yang, et al., Biomed. Mater. 17 (2022) 025005.
[9] Y. Wang, L. Su, Y. Hou, et al., Macromol. Biosci. 22 (2022) 2100352.
[10] J. Zhong, H. Wang, K. Yang, et al., Bioact. Mater. 9 (2022) 523–540.
[11] M. Hosseini, A. Shafiee, Small 17 (2021) 2101384.
[12] X. Wang, F. Lv, T. Li, et al., ACS Nano 11 (2017) 11337–11349.
[13] X. Liu, M. Wu, M. Wang, et al., Adv. Mater. 34 (2022) 2109010.
[14] S. Du, N. Zhou, G. Xie, et al., Nano Energy 85 (2021) 106004.
[15] R. Yuan, N. Yang, S. Fan, et al., Small 17 (2021) 2103997.
[16] O. Castaño, S. PérezAmodio, C. NavarroRequena, M.Á. MateosTimoneda, E. Engel, Adv. Drug Deliv. Rev. 129 (2018) 95–117.
[17] R.E. Jones, D.S. Foster, M.T. Longaker, JAMA 320 (2018) 1481–1482.
[18] J. Zhang, Y. Zheng, J. Lee, et al., Nat. Commun. 12 (2021) 1670.
[19] P.K. Gajendrareddy, C.K. Sen, M.P. Horan, P.T. Marucha, Brain Behav. Immun. 19 (2005) 217–222.
[20] J. Lu, Y. Chen, M. Ding, et al., Carbohydr. Polym. 277 (2022) 118871.
[21] X. Wang, J. Qi, W. Zhang, et al., Int. J. Biol. Macromol. 187 (2021) 91–104.
[22] S. Radmanesh, S. Shabangiz, N. Koupaei, S.A. HassanzadehTabrizi, J. Polym. Res. 29 (2022) 50.
[23] Y. Li, H. Zheng, Y. Liang, et al., Chin. Chem. Lett. 33 (2022) 5030–5034.
[24] Y.K. Li, H.Y. Zheng, Y.X. Liang, et al., Chin. Chem. Lett. 33 (2022) 5030–5034.
[25] C. Wang, J. Chen, X. Yue, et al., AAPS PharmSciTech 23 (2022) 68.
[26] J. Li, X. Liu, L. Tan, et al., Nat. Commun. 10 (2019) 4490.
[27] Y. Li, R. Fu, Z. Duan, C. Zhu, D. Fan, Colloids Surf. B 210 (2022) 112230.
[28] M. Hou, Y. Zhong, L. Zhang, et al., Chin. Chem. Lett. 32 (2021) 1055–1060.
[29] C. Yang, S. Shang, D. Shou, et al., Mater. Chem. Phys. 277 (2022) 125484.
[30] G.S. de Souza, L. de Jesus Sonego, A.C. Santos Mundim, et al., Peptides 148 (2022) 170707.
[31] N. Guo, Y. Xia, Y. Duan, et al., Chin. Chem. Lett. 34 (2023) 107542.
[32] Y. Liang, Y. Liang, H. Zhang, B. Guo, Asian J. Pharm. Sci. 17 (2022) 353–384.
[33] Y. Yu, P. Li, C. Zhu, et al., Adv. Funct. Mater. 29 (2019) 1904402.
[34] D. Hu, L. Zou, B. Li, et al., ACS Biomater. Sci. Eng. 5 (2019) 5169–5179.
[35] Y. Xiang, C. Mao, X. Liu, et al., Small 15 (2019) 1900322.
[36] Y. Liu, Y. Xi, J. Zhao, et al., Chem. Eng. J. 375 (2019) 122048.
[37] B. Zhuang, T. Chen, Y. Huang, Z. Xiao, Y. Jin, Acta Pharm. Sin. B 12 (2022) 1447–1459.
[38] X. Qi, Y. Huang, S. You, et al., Adv. Sci. 9 (2022) 2106015.
[39] S. Chen, S. Liu, L. Zhang, et al., Chem. Eng. J. 399 (2020) 125795.
[40] M. Suneetha, K.M. Rao, S.S. Han, ACS Omega 4 (2019) 12647–12656.
[41] F. Zhou, Y. Yang, W. Zhang, et al., Appl. Mater. Today 26 (2022) 101290.
[42] Y. Ren, H. Liu, X. Liu, et al., Cell Rep. Phys. Sci. 1 (2020) 100245.
[43] S.P. Miguel, A.F. Moreira, I.J. Correia, Int. J. Biol. Macromol. 127 (2019) 460–475.
[44] K. Zheng, Y. Tong, S. Zhang, et al., Adv. Funct. Mater. 31 (2021) 2102599.
[45] J. Qu, X. Zhao, Y. Liang, et al., Biomaterials 183 (2018) 185–199.
[46] L. Han, M. Wang, P. Li, et al., ACS Appl. Mater. Interfaces 10 (2018) 28015–28026.
[47] L.M.Y. Yu, K. Kazazian, M.S. Shoichet, J. Biomed. Mater. Res. Part A 82A (2007) 243–255.
[48] O.M. Kolawole, W.M. Lau, V.V. Khutoryanskiy, Int. J. Pharm. 550 (2018) 123–129.
[49] Y.Y. Yeh, Y.T. Tsai, C.Y. Wu, et al., Macromol. Biosci. 22 (2022) 2100477.
[50] Z. Zou, L. Wang, Z. Zhou, et al., Bioact. Mater. 6 (2021) 1839–1851.
[51] X. Zhao, Y. Liang, B. Guo, et al., Chem. Eng. J. 403 (2021) 126329.
[52] L. Yuan, Y. Wu, Q.s. Gu, et al., Int. J. Biol. Macromol. 96 (2017) 569–577.
[53] A. Lejardi, R. Hernández, M. Criado, et al., Carbohydr. Polym. 103 (2014) 267–273.
[54] Z. Ling, Z. Chen, J. Deng, et al., Chem. Eng. J. 420 (2021) 130302.
[55] Y. Liang, X. Zhao, T. Hu, Y. Han, B. Guo, J. Colloid Interface Sci. 556 (2019) 514–528.
[56] X. Jing, H.Y. Mi, B.N. Napiwocki, X.F. Peng, L.S. Turng, Carbon 125 (2017) 557–570.
[57] Y. Liang, X. Zhao, T. Hu, et al., Small 15 (2019) 1900046.
[58] Y.L. Mao, Z.Y. Xu, Z.H. He, J. Wang, Z. Zhu, Chin. Chem. Lett. 34 (2023) 107461.
[59] Y. Chen, Y. Qiu, Q. Wang, et al., Chem. Eng. J. 399 (2020) 125668.
[60] C. Chen, P. Zhou, C. Huang, et al., Carbohydr. Polym. 273 (2021) 118557.
[61] T. Liu, G. Liu, J. Zhang, et al., Chin. Chem. Lett. 33 (2022) 1880–1884.
[62] R. Gharibi, H. Yeganeh, A. RezapourLactoee, Z.M. Hassan, ACS Appl. Mater. Interfaces 7 (2015) 24296–24311.
[63] B. Kim, B. Kang, T.P. Vales, et al., Macromol. Res. 26 (2018) 35–39.
[64] P. Tang, L. Han, P. Li, et al., ACS Appl. Mater. Interfaces 11 (2019) 7703–7714.
[65] Y. Liang, Z. Li, Y. Huang, R. Yu, B. Guo, ACS Nano 15 (2021) 7078–7093.
[66] Q. Pang, K. Wu, Z. Jiang, et al., Macromol. Biosci. 22 (2022) 2100386.
[67] C. Guo, J. Zhang, X. Feng, et al., Chin. Chem. Lett. 33 (2022) 2975–2981.
[68] L. Fan, Z. He, X. Peng, et al., ACS Appl. Mater. Interfaces 13 (2021) 53541–53552.
[69] Y. Fu, L. Yang, J. Zhang, et al., Mater. Horiz. 8 (2021) 1618–1633.
[70] Y. Kong, Z. Hou, L. Zhou, et al., ACS Biomater. Sci. Eng. 7 (2021) 335–349.
[71] P.K. Sharma, M. Halder, U. Srivastava, Y. Singh, ACS Appl. Bio Mater. 2 (2019) 5313–5322.
[72] H. Huang, D. He, X. Liao, H. Zeng, Z. Fan, Mater. Sci. Eng. C 129 (2021) 112395.
[73] A.G. Rusu, A.P. Chiriac, L.E. Nita, et al., Int. J. Biol. Macromol. 132 (2019) 374–384.
[74] N. Pettinelli, S. RodríguezLlamazares, V. Abella, et al., Mater. Sci. Eng. C 96 (2019) 583–590.
[75] K. Bankoti, A.P. Rameshbabu, S. Datta, et al., J. Mater. Chem. B 8 (2020) 9277–9294.
[76] X. Zhao, H. Wu, B. Guo, et al., Biomaterials 122 (2017) 34–47.
[77] Y. Liang, J. He, B. Guo, ACS Nano 15 (2021) 12687–12722.
[78] J. Wu, Z. Xiao, A. Chen, et al., Acta Biomater. 71 (2018) 293–305.
[79] Y. Shen, G. Xu, H. Huang, et al., ACS Nano 15 (2021) 6352–6368.
[80] X. Chen, X. Cao, H. Jiang, et al., Molecules 23 (2018) 2611.
[81] W. Zhou, L. Zi, Y. Cen, C. You, M. Tian, Front. Bioeng. Biotechnol. 8 (2020) 417.
[82] E.Y.X. Loh, N. Mohamad, M.B. Fauzi, et al., Sci. Rep. 8 (2018) 2875.
[83] S. Korntner, C. Lehner, R. Gehwolf, et al., Adv. Drug Deliv. Rev. 146 (2019) 170–189.
[84] K. Wu, M. Fu, Y. Zhao, et al., Bioact. Mater. 20 (2023) 93–110.
[85] A.C. Strömdahl, L. Ignatowicz, G. Petruk, et al., Acta Biomater. 128 (2021) 314–331.
[86] S. Yao, Y. Zhao, Y. Xu, et al., Adv. Healthcare Mater. 11 (2022) 2200516.